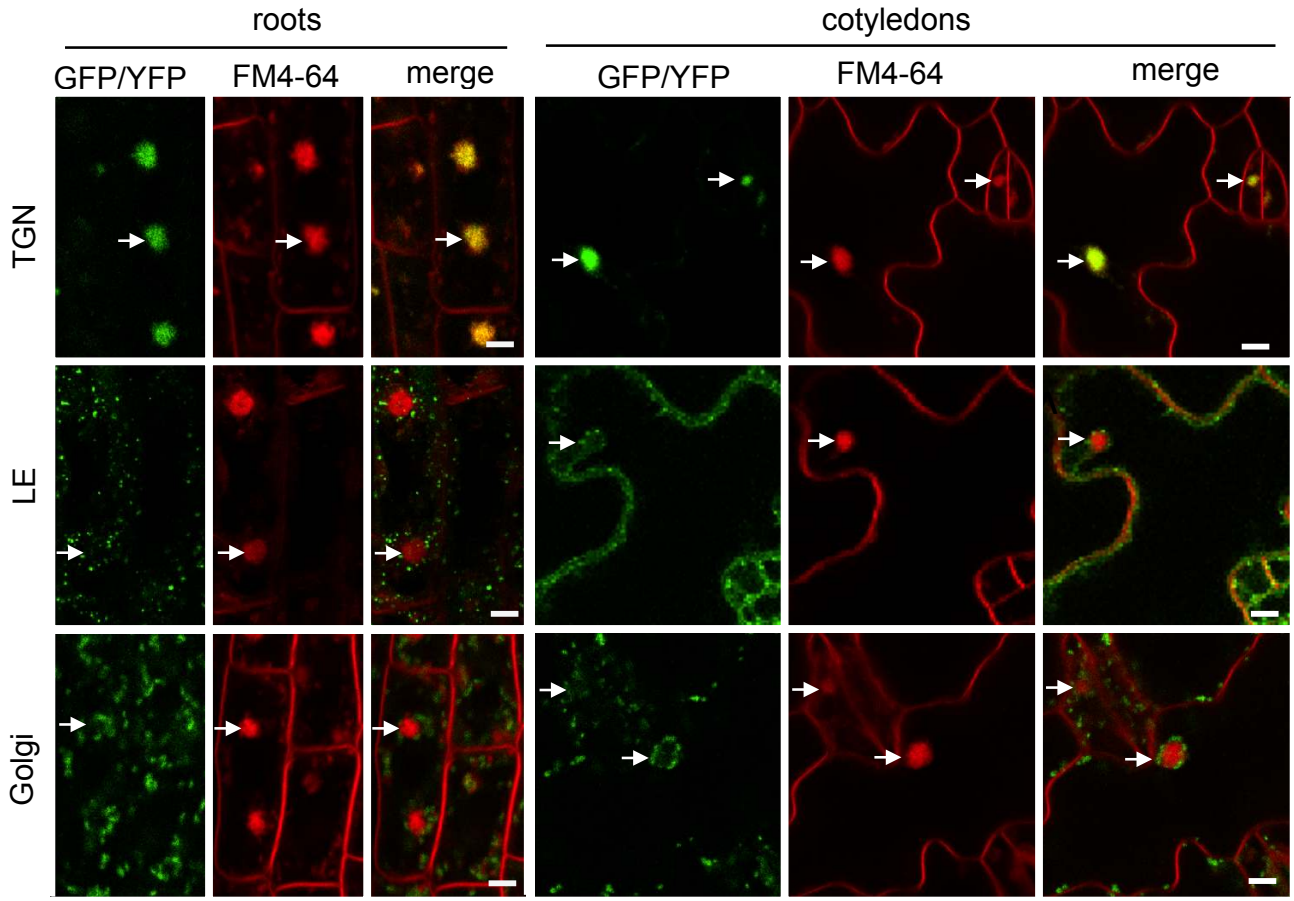

Figure S1. BFA-body formation in Arabidopsis root and cotyledon cells. Standard confocal micrographs of Arabidopsis transgenic lines expressing the EE/TGN marker VTI12-YFP, the LE/MVB marker GFP-FYVE, and the Golgi marker SYP32-YFP show optical sections of roots and cotyledons stained with the endocytic tracer FM4-64 upon BFA treatments. GFP/YFP-tagged markers are shown in green, FM4-64 staining in red and co-localisation in yellow. Arrows point at BFA compartments. Bar =10 μm.

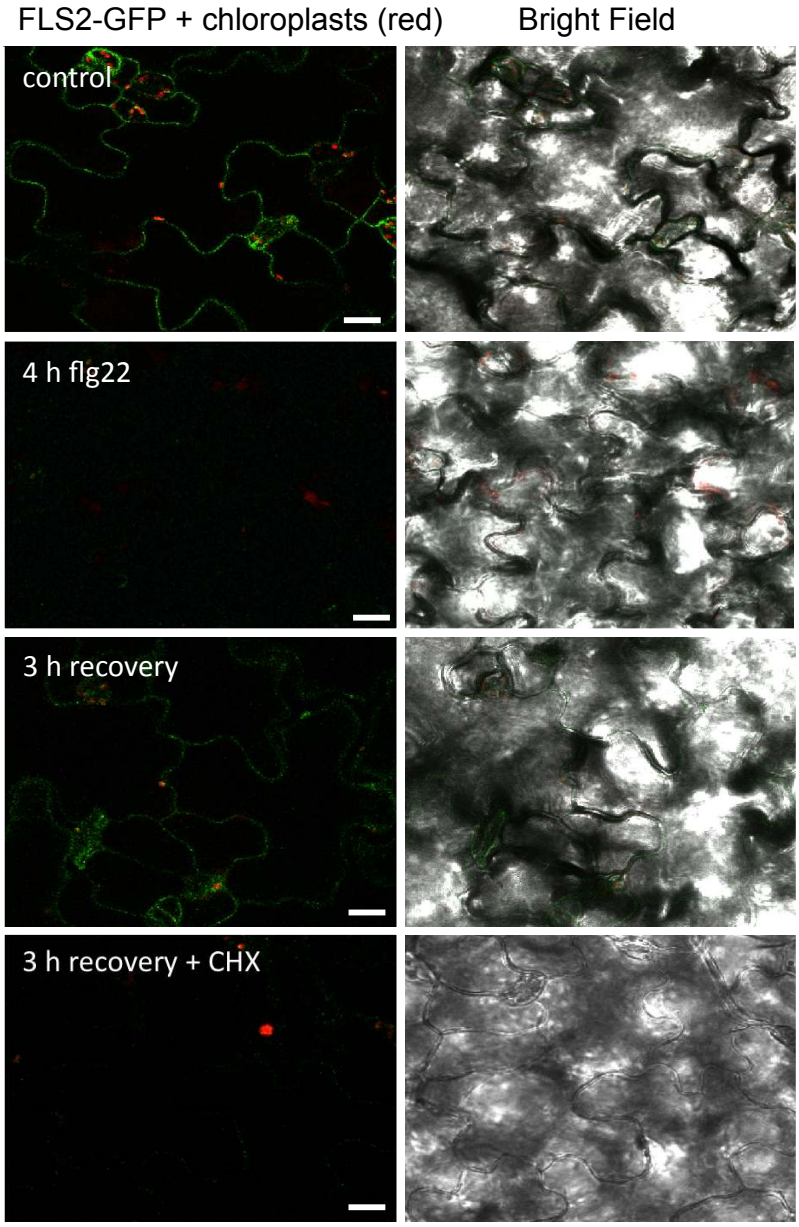

Figure S2. Cycloheximide effects in cotyledon cells of FLS2-GFP plants. Standard confocal micrographs of *Arabidopsis* transgenic lines expressing FLS2-GFP show optical sections of cotyledons under the indicated treatments. FLS2-GFP is shown in green, chlorophyll autofluorescence in red and is overlayed with bright field images. Under control conditions, FLS2-GFP signals were detected at the plasma membrane, which was depleted after 4 h of flg22 treatment and recovered after 3 h of non-treatment. No FLS2-GFP signal was recovered at the plasma membrane in the presence of cyclohexamide (CHX). Bar = 20 µm.

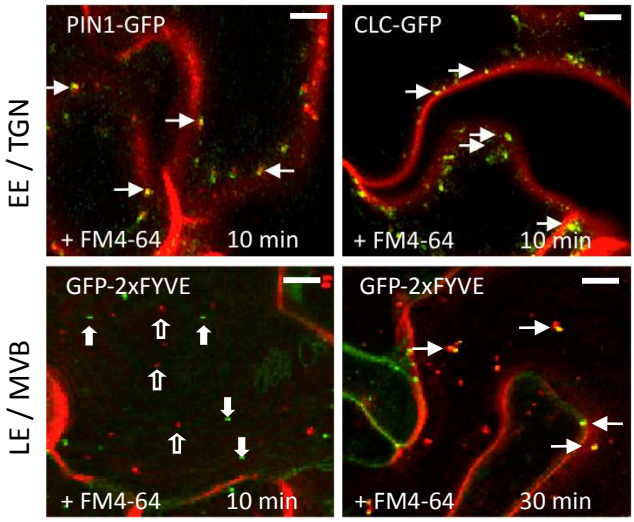

Figure S3. FM4-64 endocytic tracing in Arabidopsis cotyledons. Standard confocal micrographs of *Arabidopsis* transgenic lines expressing the known EE/TGN markers PIN1-GFP and CLC-GFP as well as the LE/MVB marker GFP-2xFYVE show optical sections of cotyledons stained with the endocytic tracer at the indicated time points. GFP-tagged markers are shown in green, FM4-64 staining in red and co-localisation in yellow. Arrows point at co-localised compartments; filled and empty block arrows point at distinct GFP-2xFYVE and FM4-64 compartments, respectively. Bar = 10 µm.

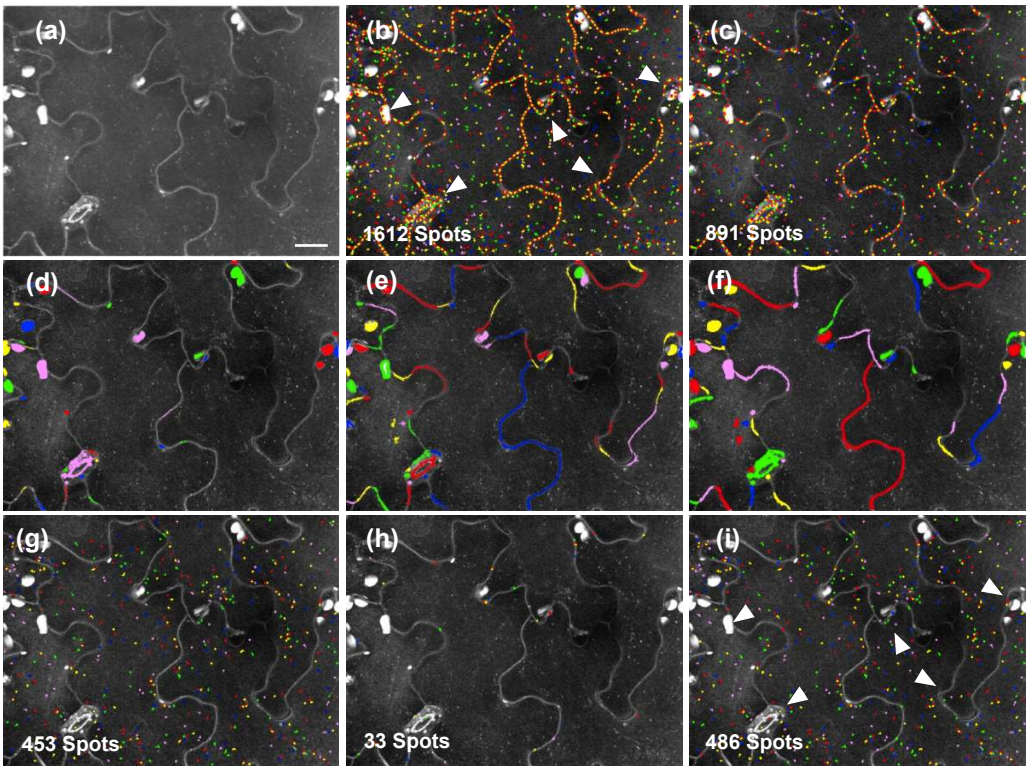

Figure S4. Features of the EndomembraneQuantifier script

(a) Maximum projection of 21 optical planes merged into a pseudo 2D projection image. Bar = 30 µm.

(b) Computational detection using the Endomembrane script. Endomembrane compartments (spots) are recognised and presented by random coloured circles. White arrowheads point at false detected spots, caused by high intensity areas such as cell wall, stomata, chloroplasts, and dust.

(c) Newly developed filtering system screens out preliminary spot candidates based on their roundness, intensity, area, length and width (for details see Supplemental Dataset 1).

(d), (e), (f) A dynamic mask function identifies "real" spots by detecting high intensity regions on maximum projection images and categorising the remaining spots into two groups, dark-region and bright-region.

(g), (h) The contrast between the intensity of a spot-like object and its surrounding area is calculated by a filtering system and genuine spots from two regional groups are selected according to their contrast values (for details see Supplemental Dataset 1).

(i) Refined spots are saved in an objects list for final output. Most of the false detected spots are removed by applying these filtering systems (white arrowhead-spots before filtering), genuine spots on the cell wall remain in the final output.

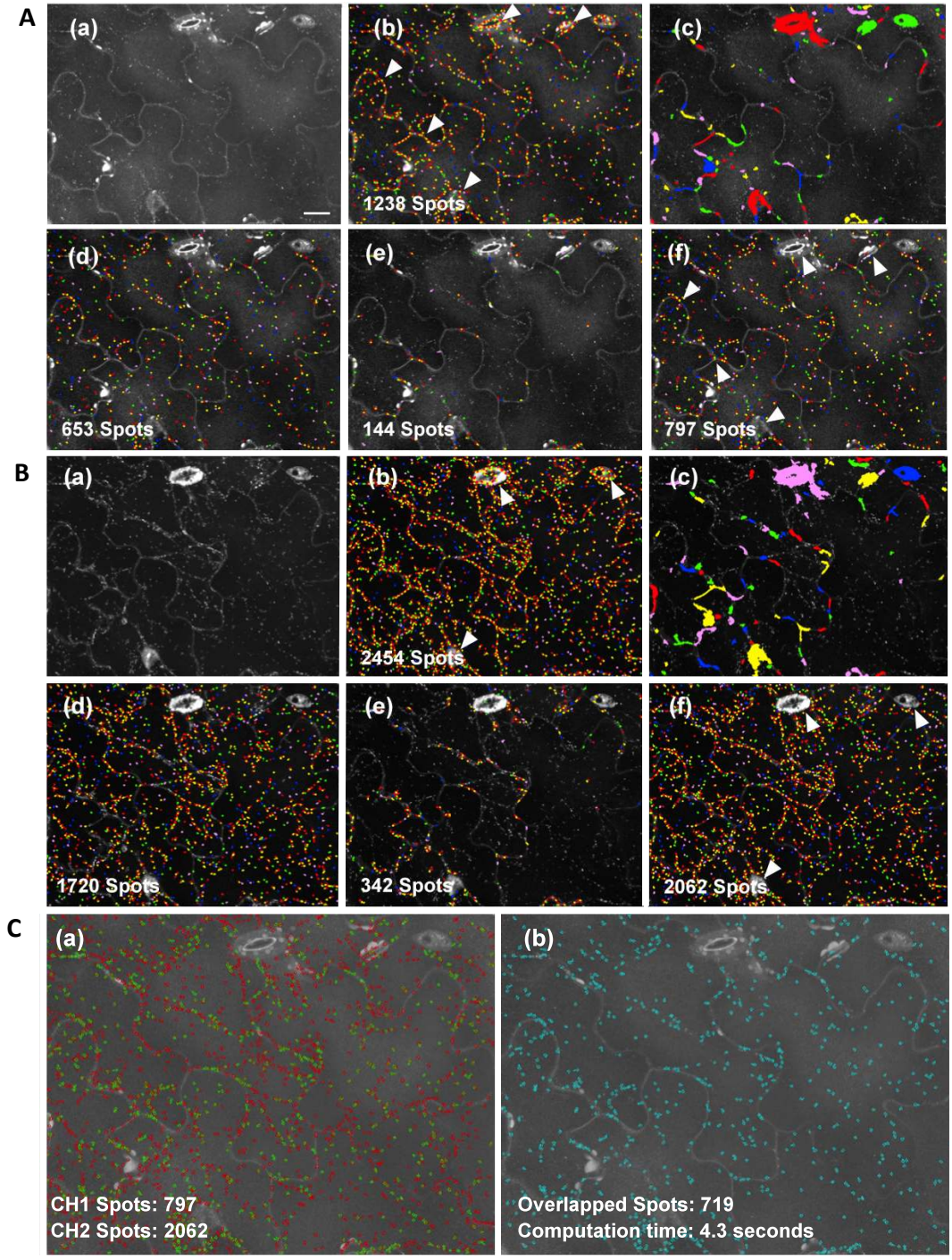
A
(a)
(b)
1238 Spots
(c)
(d)
653 Spots
(e)
144 Spots
(f)
797 Spots
B
(a)
(b)
2454 Spots
(c)
(d)
1720 Spots
(e)
342 Spots
(f)
2062 Spots
C
(a)
CH1 Spots: 797
CH2 Spots: 2062
(b)
Overlapped Spots: 719
Computation time: 4.3 seconds

Figure S5. Features of the EndomembraneCoLocQuantifier script

A) Channel one (GFP):

(a) Maximum projection of 21 optical planes merged into a pseudo 2D projection image. Bar = 30 µm.

(b) Computational detection using the Endomembrane script. Endomembrane compartments (spots) are recognised and presented by random colored circles. White arrowheads point at false detected spots, caused by high intensity areas such as cell wall, stomata, chloroplasts, and dust.

(c) A dynamic mask function identifies "real" spots by calculating high intensity regions on the maximum projection image and remaining spots are categorized into two groups, dark-region and bright-region.

(d), (e) Spots belonging to two regional groups are filtered according to their roundness, intensity, area, length, and width. Computation results are saved in an objects list. The contrast between the intensity of a spot-like object and ıts surrounding area is calculated by a filtering system and genuine spots from two groups are selected according to their contrast values (for details see Supplemental Dataset 2 online).

(f) Selected channel-one spots are saved in an objects list as final output. Most of the false detected spots are removed by using the filtering systems (white arrowhead-spots before filtering).

B) Channel two (RFP):

(a) Maximum projection of 21 optical planes merged into a pseudo 2D projection image.

(b) Computational detection using the Endomembrane script[41] (c) A dynamic mask function divides the initial spots into two groups, bright-region and dark-region.

(d), (e) Spots are filtered according to their roundness, intensity, area, length, and width; Computation results are saved in an objects list. The contrast value between the intensity of a spot-like object and its surrounding area is calculated by a filtering system.

(f) Filtered channel-two spots are saved in an objects list for final output. Most of the false detected spots are removed with the filtering systems (white arrowhead-spots before filtering).

C) Co-localisation algorithm:

(a)

Co-localisation procedure:

(a) The co-localisation procedure combines channel-one spots objects list (GFP, Figure S5A) with the channel-two objects list (RFP, Figure S5B). Spots from two channels are placed on a channel-one maximum projection image.

(b) If a channel-one spot boundary touches or fully contains one or more channel-two spot boundaries, the spot is considered co-localised. The total number of overlapped spots is then calculated (for a detailed calculation see Supplemental Dataset 2 online).

A

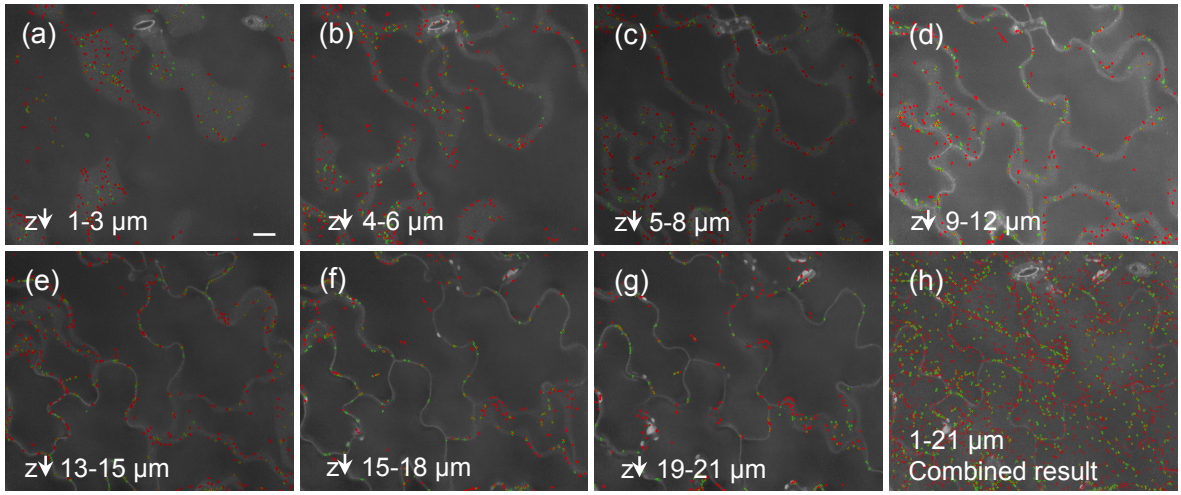

B

n=15	Maximum projection detection	Z-planes detection	Relative Error	Student t-test: p -value
Overlapped spots	603±96	630±82	±4.261%	0.203

C

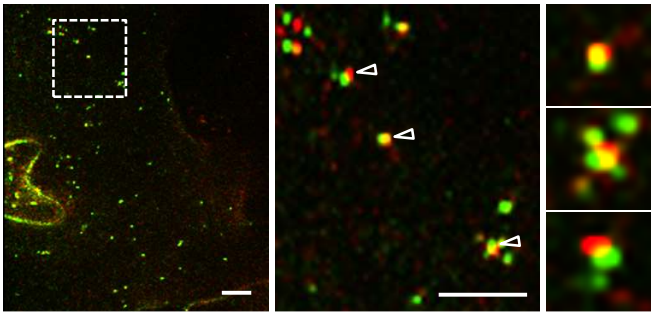

Figure S6. Evaluation of the EndomembraneCoLocQuantifier

A) To compare the difference between endosome co-localisation based on maximum projection detection and z-planes detection (identifying spots slice by slice), we sequentially combined three optical planes and generated seven pseudo 2D slices from a 21-plane image, which were then analysed with the EndomembraneCoLocQuantifier script. Images (a-g) show overlapping endosomes detected from the seven merged slices (channel 1 spots are colored green and channel 2 spots are coloured red; each depth 3 µm, total 21 µm). Image (h) shows the combined result of overlapped endosomes from the seven slices, which is superimposed on a maximum projection. Bar = 30 µm.

B) Comparison of overlapped spots detected on maximum projection images (n = 15) to those identified in z-planes detection. The relative error between the two detections in percent is 4.261% and no significant difference could be discovered between two sets of overlapped spot numbers (p = 0.203). The time to measure co-localisation from maximum projections is 3 s per image, while it is 40 s using the z-planes detection.

C) Endosome movement within the time lapse of 120 ms of consecutive imaging. Time frame 0 is colored green and time frame 120 ms is colored red. To visualize the displacement of the same FLS2–GFP endosome within the 120 ms of time lapse, the two time frames were overlayed. Insets show co localisation in yellow of the same endosome over time. Bar = 10 µm.

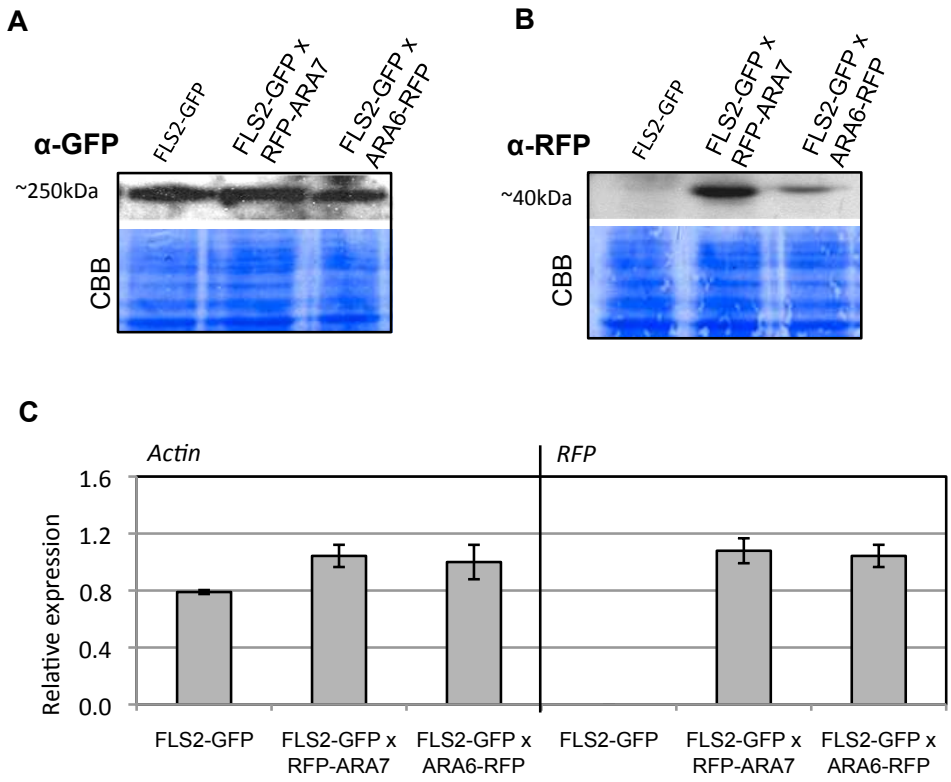

Figure S7. Expression analysis of RFP-ARA7/Rab F2b and ARA6/Rab F1-RFP transgenic lines expressing FLS2-GFP. A) FLS2-GFP protein abundance, and B) RFP-ARA7/Rab F2b and ARA6/Rab F1-RFP protein abundance as revealed by α-GFP and α-RFP immuno blot analysis from total seedling extracts. Coomassie brilliant blue (CBB) is shown as loading control. C) qRT-PCR showing relative transcript levels of *RFP-ARA7/Rab F2b* and *ARA6/Rab F1-RFP* and *Actin* as control. Error bars represent SD of three technical replicates.

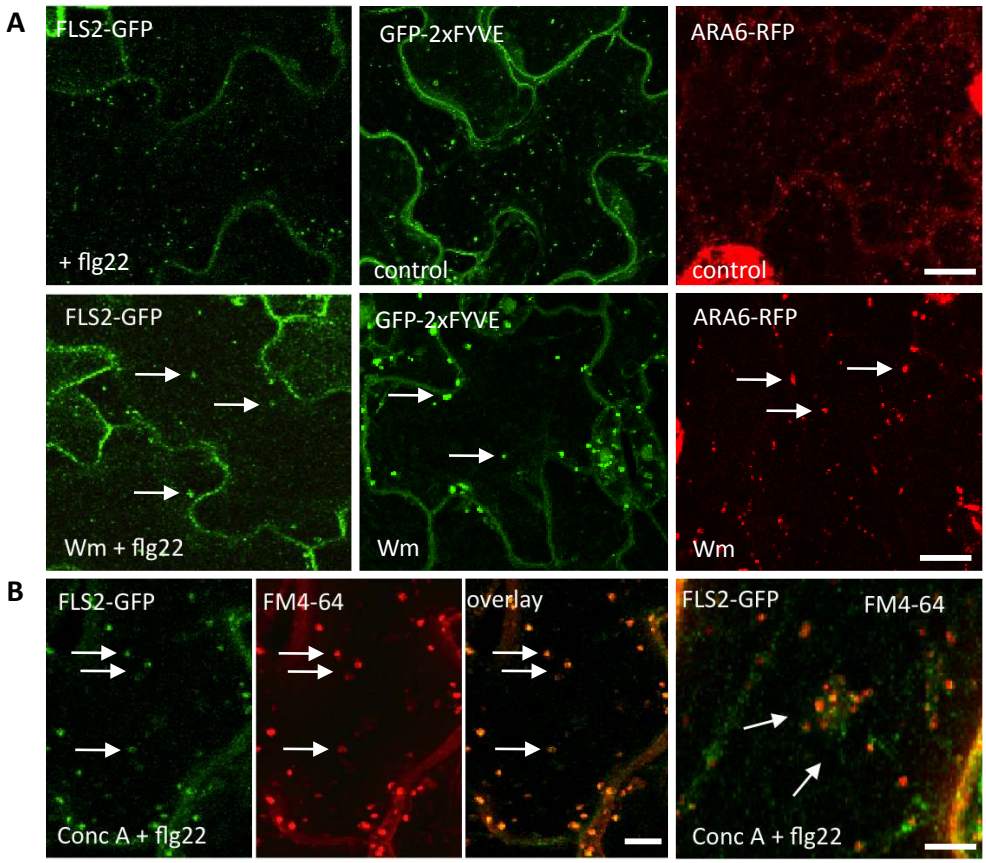

Figure S8. Effects of membrane trafficking inhibitors on known subcellular markers and FLS2-GFP. Standard confocal micrographs of *Arabidopsis* transgenic lines expressing the LE/MVB markers GFP-2xFYVE and ARA6/Rab F1-RFP, and FLS2-GFP show cotyledon epidermal cells treated with the indicated chemical inhibitors. A) Effects of Wortmannin (Wm) treatment on flg22-induced FLS2-GFP endosomes and the indicated LE/MVB markers. Arrows point at enlarged endosomal compartments. B) Effects of Concanamycin A (ConcA) treatment on flg22-induced FLS2-GFP endosomes co-stained with FM4-64. Arrows point at co-localised compartments clustering closely together. GFP-tagged markers are shown in green, RFP-tagged markers and FM4-64 staining in red and co-localised compartments in yellow. Bar = 20 µm (A); 10 µm (B).

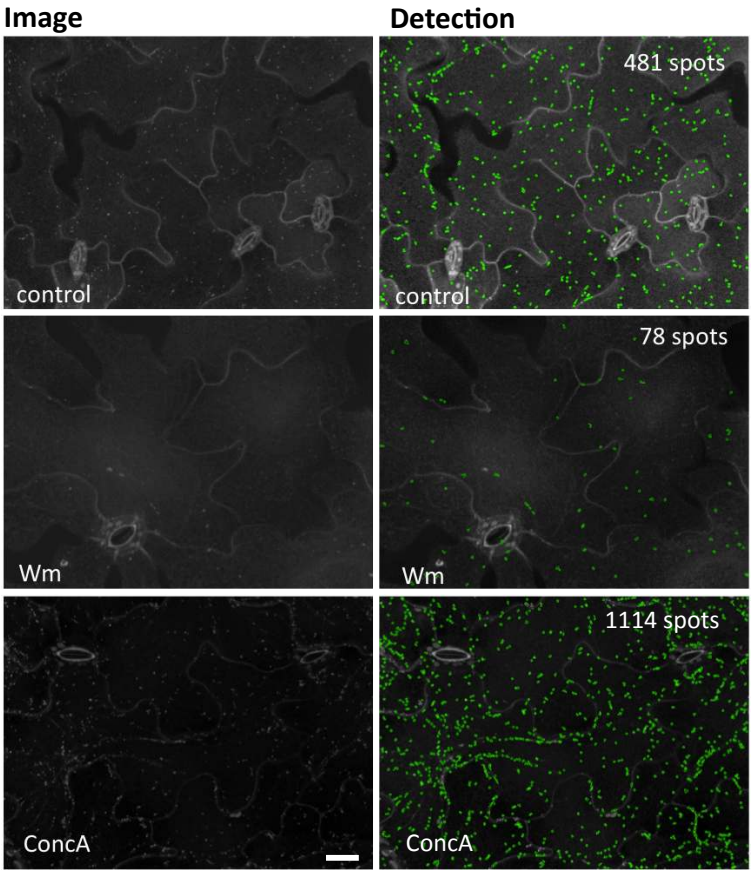

Figure S9. Quantitative imaging of FLS2 endosomes upon chemical inhibition. High-throughput confocal micrographs of *Arabidopsis* transgenic lines expressing FLS2-GFP show maximum projections of cotyledon epidermal cells treated with flg22 for 50-60 min and the indicated chemical inhibitors (images) and computational spot detection. Bar = 30 µm.

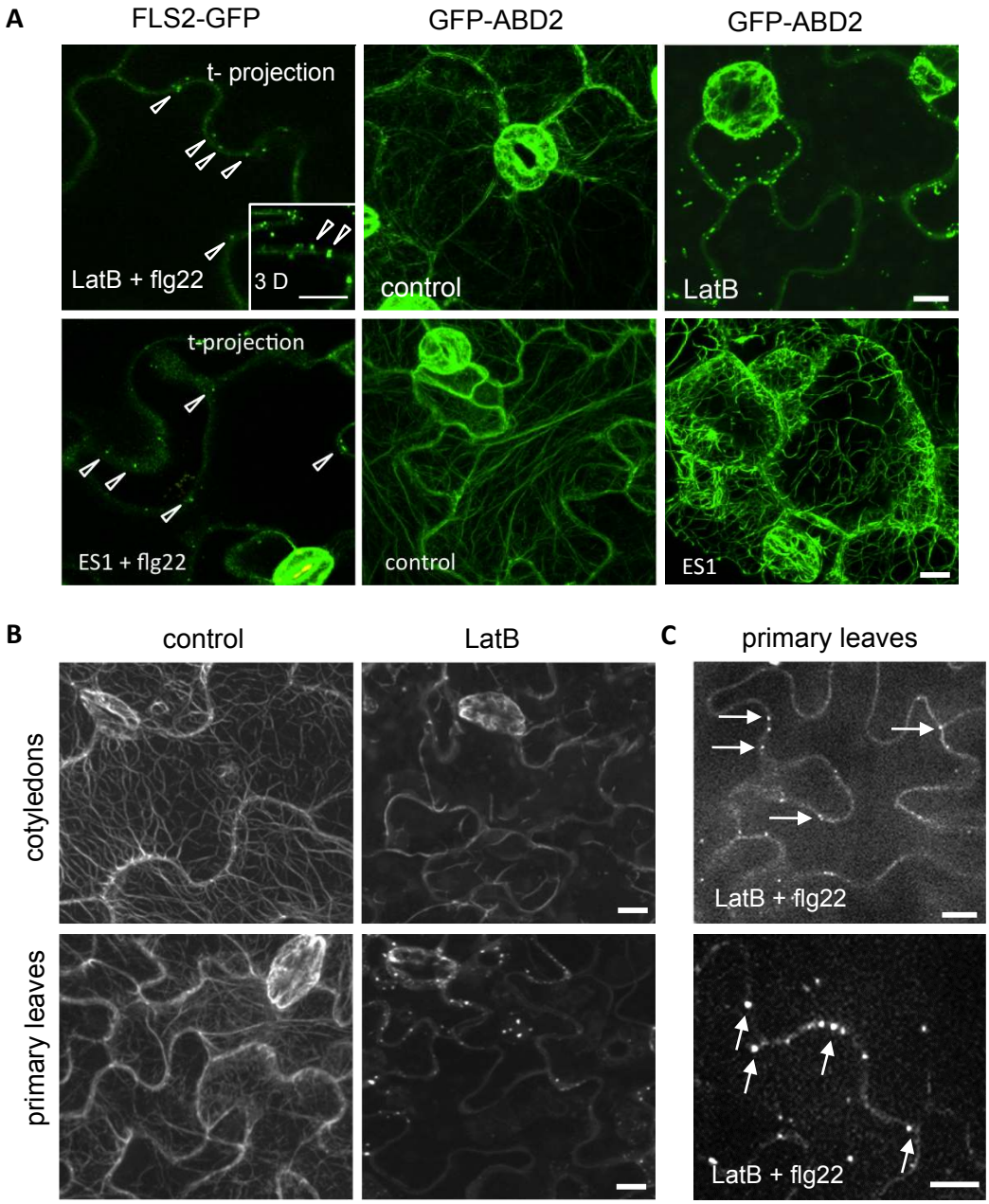

Figure S10. Effects of actin inhibitors on FLS2-GFP vesicle mobility and different leaf tissues. A) Comparison between the effects of Endosidin 1 (ES1) and Latrunculin B (LatB) on flg22-induced FLS2-GFP endosomes over time and on the actin cytoskeleton (GFP-ABD2). LatB and ES1 strongly reduce the mobility of flg22-induced FLS2-GFP endosomes. Images were taken over a 3-min time period and projected in one pseudo image. Arrows point at non-mobile FLS2-GFP endosomes, closely associated to the plasma membrane, see also inset. Both inhibitors cause severe rearrangement of the actin cytoskeleton; LatB leads to the depolymerisation of actin filaments and ES1 causes bundling and shortening of actin filaments. Bar = 20 µm. B) Comparison of LatB treatments between cotyledon and primary leaves of GFP-ABD2 - expressing plants. High-throughput confocal micrographs show strong depolymerisation of the actin network in both tissues after 1 h of LatB treatment. Bar = 20µm.
C) Effect of LatB on flg22-induced FLS2-GFP endosomes in primary leaves.
1 h pretreatment with LatB followed by a 40-min incubation with flg22 leads to internalized FLS2-GFP endosomes (arrows) close to the plasma membrane. Bar = 10 µm.

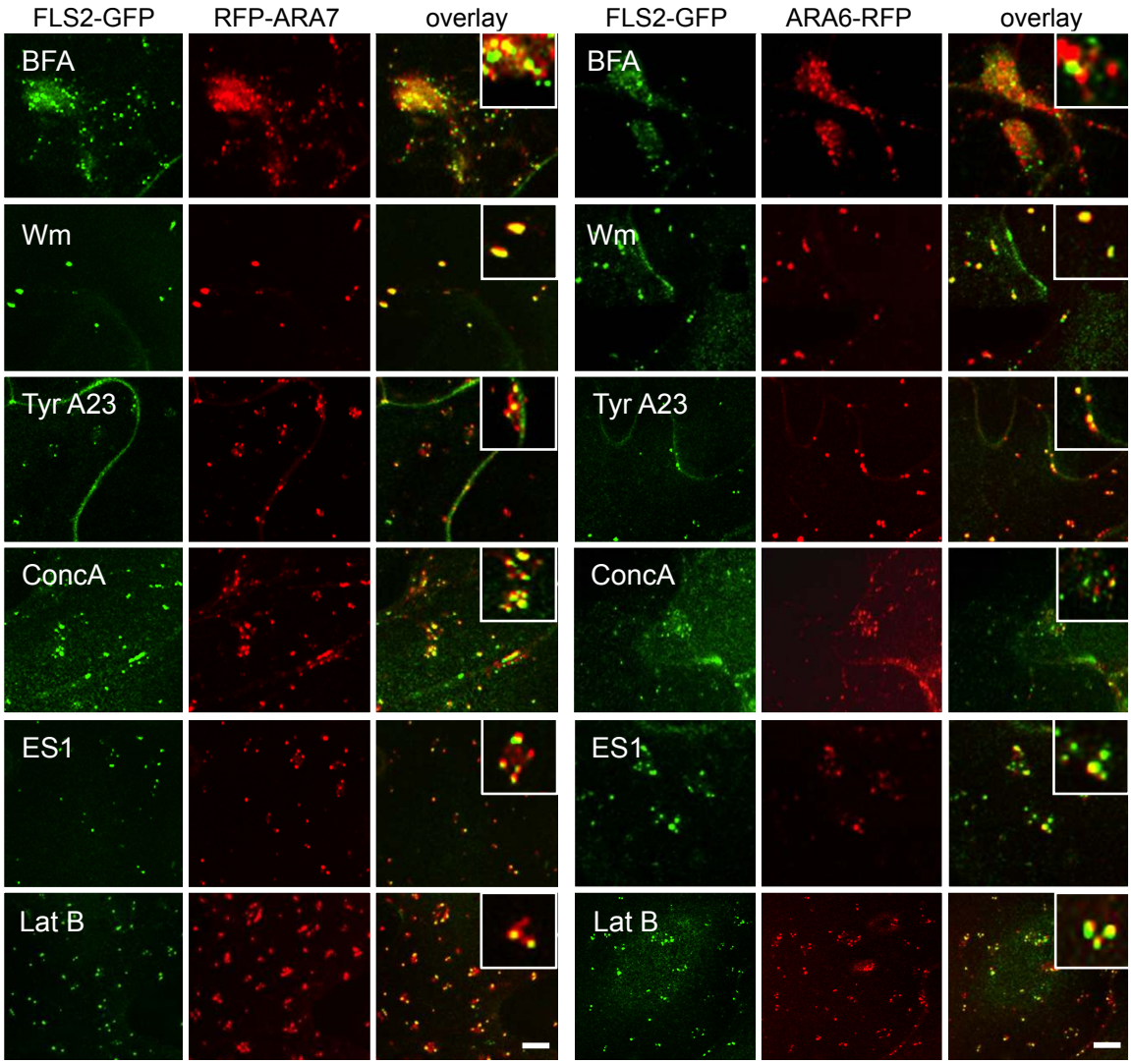

Figure S11. Effects of chemical interference on flg22-induced FLS2 endosomes co-localising to ARA7/Rab F2b and ARA6/Rab F1 and positive compartments. High-throughput confocal micrographs of *Arabidopsis* transgenic lines expressing FLS2-GFP show projections of cotyledon epidermis in the presence of flg22 and the indicated chemical inhibitors. Left panel: FLS2-GFP x RFP-ARA7/Rab F2b crossed lines; right panel: FLS2-GFP x ARA6/Rab F1-RFP crossed lines. FLS2-GFP is shown in green, RFP-ARA7/Rab F2b and ARA6/Rab F1-RFP are shown in red, overlaying compartments in yellow colour. Inset images (5 µm x 5 µm) show details. Bar = 5 µm.

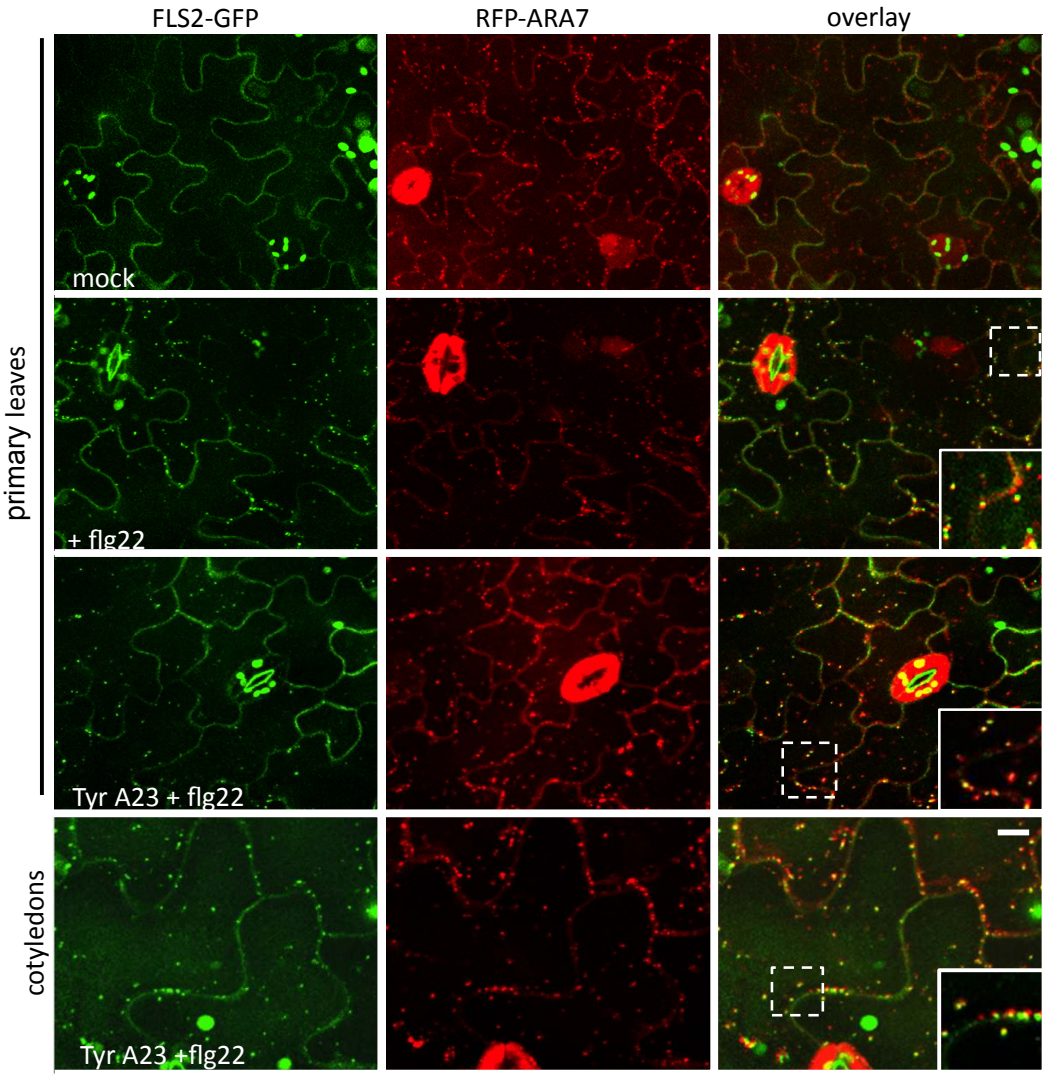

Figure S12. Effect of Tyrphostin A23 on flg22-induced FLS2-GFP endosomes co-localising to RFP-ARA7/Rab F2b positive compartments in cotyledons and primary leaves. High-throughput confocal micrographs of Arabidopsis transgenic lines expressing FLS2-GFP x RFP-ARA7/Rab F2b show projections of cotyledon epidermis in the presence of flg22 and Tyrphostin A23 (TyrA23). 1-h pre-treatment with TyrA23 followed by flg22 did not fully block flg22-induced FLS2-GFP endocytosis in cotyledon and primary leaves. Insets (20 µm x 20 µm) show details of co-localised FLS2-GFP endosomes with RFP-ARA7. Bar = 20 µm.

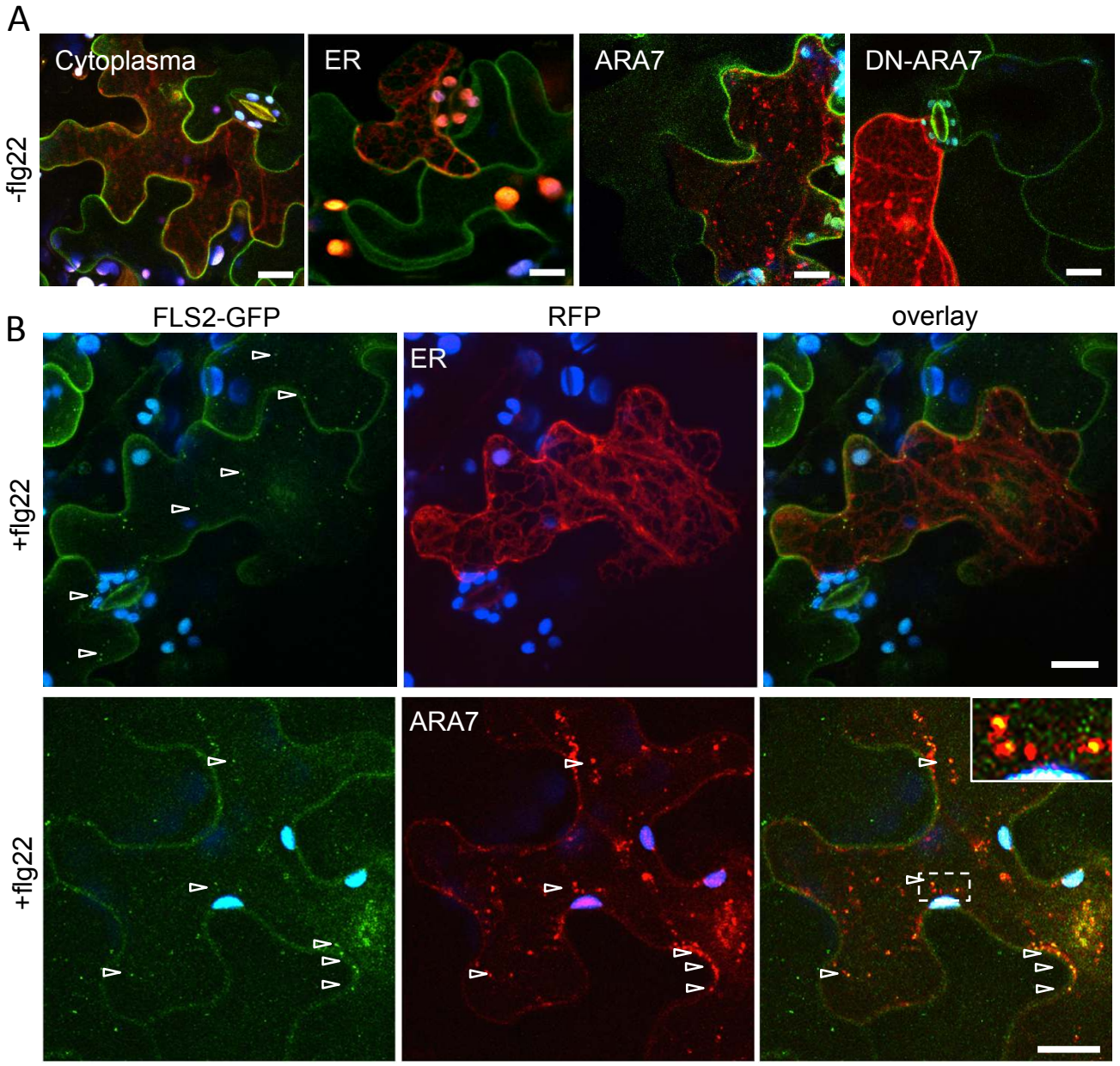

Figure S13. Flg22-induced endocytosis of FLS2-GFP and co-localization with RFP-ARA7/Rab F2b-positive compartments in transient transformed cells by particle bombardment. Standard confocal micrographs of *Arabidopsis* transgenic lines expressing FLS2-GFP show optical sections of untreated or flg22-treated leaf epidermal cells not or transiently expressing cytosolic RFP, ER-targeted RFP (ER), RFP-ARA7/Rab F2b (ARA7), or dominant-negative RFP-ARA7/Rab F2b (DN-ARA7) after particle bombardment. RFP signals indicate successful transiently transformed cells. In these cells, FLS2-GFP shows localization at the plasma membrane in the absence of flg22 trigger and at endosomes upon flg22 induction demonstrating that transient transformation by particle bombardment does not generally affect FLS2 trafficking. Flg22-induced FLS2-GFP endosomes co-localize with RFP-ARA7/Rab F2b-positive compartments indicating normal endocytic trafficking of FLS2 in transiently transformed cells. Arrowheads point at FLS2-GFP endosomes; bar = 10 µm. FLS2-GFP is shown in green, cytosolic RFP, ER-RFP, RFP-ARA7/Rab F2b, and RFP-DN-ARA7/Rab F2b in red, autofluorescence from chloroplasts is shown in blue/purple. Inset shows enlargement of boxed region and in detail endosomal co-localization of FLS2-GFP and RFP-ARA7/Rab F2b. Similar results were obtained from independently transformed cells. Bombardments with cytosolic RFP: n = 7, ER-RFP: n = 10, RFP-ARA7/Rab F2b: n = 8.

SUPPLEMENTAL TABLES

Table S1. Output parameter produced by the EndomembraneQuantifier script

Parameters exported in comma-separated value (csv) files for further statistical analysis and are highlighted in gray. Membrane compartments are called "spots" in Supplement Table S1 and S2.

No.	Output parameter	Description
1	Date of the Experiment	Date of the experiment
2	Valid Image	Valid image area (in percent) in a stack (normally 3-5 stacks in a well, which is saved in a flex file)
3	Original Number of Spots	Number of spots initially detected in a stack
4	Refined Number of Spots	Number of refined spots in a stack
5	Seconds Opera spent	Seconds that Opera has spent on imaging one stack
6	Average Intensity of Spots	Average intensity of all refined spots in a well, which includes all valid stacks
7	Average Area of Spots	Average area of all refined spots in a well (±SD)
8	Average Length of Spots	Average length of all refined spots in a well
9	Average Half Width of Spots	Average half width (radius) of all refined spots in a well
10	Average Width to Length Ratio of Spots	Average width to length ratio of all refined spots in a well (±SD)
11	Average Roundness of Spots	Average roundness of all refined spots in a well (±SD)
12	Average Contrast of Spots	Average contrast (to surrounding areas) of all refined spots in a well (±SD)
13	Average Peak Intensity of Spots	Average peak intensity of all refined spots in a well (±SD)
14	Number of Stacks	Total number of analysed stacks – excluding invalid stack(s)
15	Number of Spots in whole Well	Total number of refined spots detected in a well
16	Total seconds of Opera's analysis	Seconds that Opera has spent on imaging a well
17	Opera started analysing at:	Date and time when Opera started imaging a well
18	Opera finished analysing at:	Date and time when Opera finished imaging a well
19	Well Index	Opera reference number of a well
20	Stack Number	Index number of analysed stacks in a well
21	Opera Starting Point	Date and time when Opera started imaging a stack
22	Opera Ending Point	Date and time when Opera finished imaging a stack
23	Valid image area in percent	Valid image area in a stack (in percent)
24	Detected spots number	Number of refined spots in a stack
25[a]	Calculated spots number (100%)	Calculated spots number in a stack if the valid image area is 100 %

[a] Output field 25 was calculated as follows:

$$\text{Calculated spots number (100\%)} = (\text{Detected spots number}) * \frac{(\text{Total number of pixels in a maximum projection of a stack})}{(\text{Total number of valid pixels of the same stack})} * 100\%$$

Table S2. Output parameters produced by the EndomembraneColocQuantifier script.

Fields exported in csv files are highlighted in gray.

No.	Output parameter	Description
1	Date of the Experiment	Date of the experiment
2	Valid Image (CH1)	Is channel-one image in a stack valid? (return "true" or "false")
3	Valid Image area (in percent)	Valid image area in channel-one image in a stack
4	Total number of spots (CH1)	Number of refined spots in channel-one image
5	Number of spots in 100% image area (CH1)	Calculated spots number in channel-one image, if the valid image area is 100 %
6	Total number of spots (CH2)	Number of refined spots in channel-two image
7	Number of spots in 100% image area (CH2)	Calculated spots number in channel-two image, if the valid image area is 100 %
8	Total overlapped spots	Number of overlapped spots between channel-one and channel-two images
9	Total overlapped spots in 100% image area	Calculated overlapped spots number, if the valid image area in channel one and channel two is 100 %
10[a]	Overlap percentage	The overlap percentage in a valid stack
11	Seconds Opera spent	Seconds that Opera has spent on imaging a stack
12	Number of Stacks	Total number of valid stacks in a well
13	Average Intensity of Spots (CH1)	Average intensity of all refined channel-one spots in a well
14	Average Intensity of Spots (CH2)	Average intensity of all refined channel-two spots in a well
15	Average Area of Spots (CH1)	Average area of all refined channel-one spots in a well (±SD)
16	Average Area of Spots (CH2)	Average area of all refined channel-two spots in a well (±SD)
17	Average Length of Spots (CH1)	Average length of all channel-one spots in a well
18	Average Length of Spots (CH2)	Average length of all channel-two spots in a well
19	Average Half Width of Spots (CH1)	Average half width (radius) of all channel-one spots in a well
20	Average Half Width of Spots (CH2)	Average half width (radius) of all channel-two spots in a well
21	Average Width to Length Ratio of Spots (CH1)	Average width to length ratio of all channel-one spots in a well (±SD)
22	Average Width to Length Ratio of Spots (CH2)	Average width to length ratio of all channel-two spots in a well (±SD)
23	Average Roundness of Spots (CH1)	Average roundness of all channel-one spots in a well (±SD)
24	Average Roundness of Spots (CH2)	Average roundness of all channel-two spots in a well (±SD)
25	Average Contrast of Spots (CH1)	Average contrast (to surrounding areas) of all channel-one spots in a well (±SD)
26	Average Contrast of Spots (CH2)	Average contrast (to surrounding areas) of all channel-two spots in a well (±SD)
27	Average Peak Intensity of Spots (CH1)	Average peak intensity of all channel-one spots in a well (±SD)
28	Average Peak Intensity of Spots (CH2)	Average peak intensity of all channel-two spots in a well (±SD)
29	Total seconds of Opera's analysis	Seconds that Opera has spent on imaging a whole well
30	Opera started analysing at:	Date and time when Opera started imaging a whole well

31	Opera finished analysing at:	Date and time when Opera finished imaging a whole well
32	Well Index	Opera reference number of a well
33	Stack Number	Index number of analysed stacks in a well
34	Opera Starting Point	Date and time when Opera started imaging a stack
35	Opera Ending Point	Date and time when Opera finished imaging a stack
36	Valid image area in percent	Valid Image area in channel one
37 [b]	Calculated spots number (100%) (CH1)	Calculated spots number in channel-one image of a stack, if the valid image area is 100 %
38 [b]	Calculated spots number (100%) (CH2)	Calculated spots number in channel-two image of a stack, if the valid image area is 100 %
39 [c]	Overlapped spots number (100%)	Calculated overlapped spots number in a stack, if the valid image area in channel one and channel two is 100 %
40	Overlap percent	The overlap percentage in a valid stack

a. Output field 10 was calculated as follows:

$$\text{Overlap percent} = \frac{(\text{The number of overlapped spots detected in a stack})}{(\text{Total number of refined channel-one spots in the same stack})} * 100\%$$

b. Output fields 37 and 38 were calculated as follows:

$$\text{Calculated spots number in CH1 (100\%)} = (\text{Spots number in CH1}) * \frac{(\text{Total number of pixels in CH1's maximum projection image})}{(\text{Total number of valid pixels of CH1's image area})} * 100\%$$

$$\text{Calculated spots number in CH2 (100\%)} = (\text{Spots number in CH2}) * \frac{(\text{Total number of pixels in CH2's maximum projection image})}{(\text{Total number of valid pixels of CH1's image area})} * 100\%$$

c. Output field 39 was calculated as follows:

$$\text{Overlap spots number (100\%)} = \frac{(\text{Calculated overlapped spots number in a stack})}{(\text{Calculated channel-one spots number in the same stack})} * 100\%$$

Supplement Materials and Methods:

Protein extraction and Western blotting

Crude protein extracts generated from leaves of 21 days-old plants were separated on SDS-PAGE, blotted on PVDF membrane, and incubated with mouse α-GFP antibody (Roche, 1:1000) or rabbit α-RFP antibody (AbCam, 1:10000). The secondary antibodies (Sigma, 1:30000) were Alkaline Phosphate conjugated and the chemiluminescence signal was detected after incubation with CDP-Star (Roche). The same blot was further used for Coomassie Brilliant Blue staining and used as loading control.

RNA extraction and qRT-PCR

RNA from leaves of 21 days-old plants was extracted using the RNeasy Kit (Qiagen). 1 µg RNA was used for the reverse transcription reaction according to the Superscript II protocol (Invitrogen). After DNase treatment (TUROBO DNA-free, Applied biosystem) 50 ng cDNA was used for qRT-PCR reactions mixed with SYBR green JumpStart (Sigma) and the following primers (10 mM): mRFP-forward 5'-ATC CCC GAC TAC TTG AAG C-3' mRFP-reverse 5'-CCC ATG GTC TTC TTC TGC AT-3', U-box-forward 5'-TGC GCT GCC AGA TAA TAC ACT ATT-3'; U-box-reverse 5'-TGC TGC CCA ACA TCA GGT T-3'; Actin-2-forward 5'-GGT AAC ATT GTG CTC AGT GGT GG-'3; Actin-2-reverse 5'-AAC GAC CTT AAT CTT CAT GCT GC-3'. Amplification followed with annealing at 60°C for 15s and elongation at 72°C for 10s. Actin and U-Box was used as reference.